V International Conference on Particle-based Methods – Fundamentals and Applications
PARTICLES 2017
P. Wriggers, M. Bischoff, E. Oñate, D.R.J. Owen, & T. Zohdi (Eds)

DIRECT DETERMINATION OF GRANULAR PRESSURE IN LIQUID FLUIDIZED BEDS USING A DEM-BASED SIMULATION APPROACH

HAMED ABBASFARD[1], GEOFFREY EVANS[2] AND ROBERTO MORENO-ATANASIO[3]

[1] Chemical Engineering, The University of Newcastle
Callaghan 2308 NSW Australia
Hamed.Abbasfard@newcastle.edu.au

[2] Chemical Engineering, The University of Newcastle
Callaghan 2308 NSW Australia
Geoffrey.Evans@newcastle.edu.au

[3] Chemical Engineering, The University of Newcastle
Callaghan 2308 NSW Australia
Roberto.Moreno-Atanasio@newcastle.edu.au

Key words: Fluidized bed, DEM, Granular Pressure, Fluctuating Velocity

Abstract. In this paper, the fluidization of 8 mm glass particles in water has been simulated using a new methodology developed within the DEM framework. In this methodology, random liquid fluctuating velocities are used as direct input into the drag model. The specific aim of this study is to directly compute the granular pressure in a liquid fluidized bed. The granular pressure is defined using the particle-wall collision frequency and the corresponding particle momentum transport during the collision. Initially, we validated our model by comparing the relationship between superficial fluid velocity and bed expansion against the well-known Richardson-Zaki [1] equation. The results demonstrated a good agreement of our model. The granular pressure and temperature, as well as the particle-wall collision frequency, in the liquid fluidized bed were determined for superficial fluid velocities in the range between 0.08 and 0.32 m/s. The granular pressure exhibited a maximum (between 0.3-0.4 solid fraction) that matched the experimental measurements of Zenit et al. [2] for high inertia particles. The granular temperature also revealed a peak at a solid concentration of around 0.2 which is in line with the experimental measurements of Zivkovic et al. [3] and the model of Gervin et al. [4]. The set of the results presented in this study suggests that the approach used here is valid for obtaining the granular pressure and temperature for a wide range of volume fractions in liquid fluidized beds.

1 INTRODUCTION

The granular pressure is defined as the pressure exerted on the containing walls of the fluidized bed due to the collisions of particles with those walls. Batchelor [5] established the formulation of the mean motion of particles in a fluidized bed using a one-dimensional control volume stability analysis. All the parameters within Batchelor's model were correlated with the local solid volume fraction ε_s as well as superficial liquid velocity u_{sf}. Hence, the expression of granular pressure is defined as [5]:

$$P_p = \varepsilon_s \rho_p F(\varepsilon_s) u_{sf}^2 \tag{1}$$

where $F(\varepsilon_s)$ is some function of the solid volume fraction for two limiting cases of 0 and packed bed solid volume fraction ($\varepsilon_{sp} \approx 0.62$). Batchelor [5] suggested the simplest form of $F(\varepsilon_s)$ as:

$$F(\varepsilon_s) = \frac{\varepsilon_s}{\varepsilon_{sp}}\left(1 - \frac{\varepsilon_s}{\varepsilon_{sp}}\right) \tag{2}$$

Ding and Gidaspow [6] proposed a relation for the granular pressure based on the Kinetic Theory of Granular Flow (KTGF) as [7]:

$$P_p = \varepsilon_s \rho_p \theta [1 + 2(1 + e_n) g_0 \varepsilon_s] \tag{3}$$

where θ and g_0 are the granular temperature and radial distribution function, respectively. The granular temperature based on KTGF [7] for a three-dimensional flowing granular material is defined as:

$$\theta = \frac{1}{3}\overline{v^2} \tag{4}$$

where $\overline{v^2}$ is the mean value of the squares of fluctuating velocities. The coefficient of restitution, e_n, is the ratio of the impact velocity to the rebound velocity. The square of the restitution coefficient is directly proportional to the loss of kinetic energy during inelastic collisions due to damping effect [8]. The concept of the radial distribution function, g_0, is like $F(\varepsilon_s)$ used by Batchelor [5] and some different representations of it are available in literature [9-11]. We determined the granular pressure using the form of the radial distribution function proposed by Bagnold [9] as:

$$g_0 = \left[1 - \left(\frac{\varepsilon_s}{\varepsilon_{sp}}\right)^{\frac{1}{3}}\right]^{-1} \tag{5}$$

Wang and Ge [12] presented a mathematical model based on energy balance analysis to predict the granular pressure in fluidized beds of high particle inertia which is defined as:

$$P_p = 2(1 + e_n)\varepsilon_s^2 \rho_p \theta g_0 \tag{6}$$

where all parameters are the same and determined similarly as per Eq. 3.

In this paper, we are aiming at the computation of the granular pressure in a liquid fluidized bed using DEM. We have developed a new methodology to simulate the random motion of the particles influenced by the random fluctuating liquid velocity field incorporated into the drag force. A methodology for directly defining of the granular pressure based on the momentum transport during the particle-wall collision and the corresponding frequency has been presented. The simulation results for the granular pressure has been compared to the correlations available in the literature. The collision-wall frequency as well as the granular temperature in the liquid fluidized bed have also been reported here.

2 MODELING

Forces acting on the particle i are gravity, buoyancy, contact and drag, as:

$$\sum \overrightarrow{F_i} = \overrightarrow{F_{gb}} + \overrightarrow{F_c} + \overrightarrow{F_d} \tag{7}$$

The combined equation used for the gravity and buoyancy forces (in z direction) is:

$$F_{gb,z} = gV_p(\ \rho_L - \rho_p) \tag{8}$$

where V_p is the particle volume. In Eq. 1, $\overrightarrow{F_c}$ is the contact force. The soft sphere model was used to simulate particle-particle and particle-wall collisions [13]. The dominant fluid-particle interaction forces which are considered in this work are drag ($\overrightarrow{F_d}$) and buoyancy ($\overrightarrow{F_b}$). The drag model introduced by Di Felice [14] is used in Eq. 7 as it provides a smooth dependency of the drag force over the entire range of volume fractions [15].

A finite difference form of Newton's second law is used in DEM to determine particle's position, velocity and acceleration in each time step [8]. The new position of the particle centre after each time step can be found as:

$$\overrightarrow{S_i}(t + \Delta t) = \overrightarrow{S_i}(t) + \overrightarrow{v_i}(t)\Delta t + 0.5\frac{\sum \overrightarrow{F_i}(t)}{m_i}\Delta t^2 \tag{9}$$

where $\overrightarrow{v_i}(t)$ is the instantaneous particle velocity.

The fluid instantaneous fluctuating velocity used in the drag model is defined as:

$$\vec{u}(t) = \vec{\bar{u}} + \vec{\acute{u}}(t) \tag{10}$$

The local mean fluid velocity, $\vec{\bar{u}}$, in radial (x and y) direction is zero due to cylindrical symmetry. However, the mean value for the axial direction is equal to the interstitial fluid velocity (u_i) which is related to the local fluid volume fraction as:

$$\bar{u}_z = u_i = \frac{u_{sf}}{\varepsilon_{L,z}} \tag{11}$$

where u_{sf} is fluid superficial velocity and ε_L is the local liquid volume fraction.

Based on the Kinetic Theory of Granular Flow (KTGF), particle velocity can take random values in fluidized beds in both direction and magnitude [16, 17]. It is also believed that those random velocities follow a Gaussian-type Probability Distribution Function (PDF) in any direction [18-20]. As the particle constantly exchange momentum with the surrounding, liquid velocity values should also be random and fluctuating and following a Gaussian PDF with a mean value and standard deviation in any direction. The standard deviation of the fluctuating liquid velocity is the root mean squared of the instantaneous fluctuating velocity, u_{rms}.

Based on turbulence theory [21], the influence of fluid turbulence on particle motion is described by [22]:

$$u_{rms}{}^{2} = \left(1 + \frac{\tau_p}{T_L}\right)\overline{v^2} \tag{12}$$

where T_L and τ_p are the time scale of the fluid and particles, respectively. In an isotropic turbulence, the fluid time scale can be defined as $T_L = l/u_{rms}$ where l is the turbulence length scale [23]. Therefore, Eq. 12 can be written as:

$$u_{rms}{}^{2} - \frac{\overline{v^2}\tau_p}{l}u_{rms} - \overline{v^2} = 0 \tag{13}$$

A relation for the particle time scale (relaxation time) was proposed by Bel F'dhila and Simonin [24] as:

$$\tau_p = \frac{\rho_p/\rho_L + C_A}{(3/4)\overline{C_d}/d_p\, u_t} \tag{14}$$

where C_A is the added mass coefficient and equal to 0.5 [25].

For the average particle speed Duris et al. [20] presented an empirical equation based on experimental measurements in a liquid fluidized bed:

$$\overline{v} = v_t\left[8.486\left(Re_t\left(\frac{\mu}{\mu_w}\right)^{1.19}\right)^{-0.636}\left(\frac{u_{sf} - u_{mf}}{u}\right)\varepsilon_s^{0.5}\right]^{2/3} \tag{15}$$

and based on KTGF, we have [7]:

$$\overline{v^2} = (1.086\overline{v})^2 = 1.1794\overline{v}^2 \tag{16}$$

where v_t, Re_t, μ_w and u_{mf} are particle terminal velocity, particle Reynolds number based on terminal velocity, viscosity of water and fluid minimum fluidization velocity, respectively. The terminal and minimum fluidization velocities are determined from the correlations proposed by Loli et al. [26] and Wen and Yu [27], respectively.

As can be seen in Eq. 15, $\overline{v}$ is a function of the superficial fluid velocity, u_{sf}, and solid fraction, ε_s where the former is an input parameter and the latter can be defined using DEM. Therefore, the u_{rms}, which represents the level of liquid fluctuations, can be defined by solving the quadratic Eq. 13.

3 METHODOLOGY

3.1 Numerical simulation

Initially, particles were randomly positioned without overlapping in the simulation domain, which is a cylindrical column. The domain was divided into several cells (20-30 depending on bed height) along the axis of the column as shown in figure 1. Each cell height was always slightly larger than the smallest particle diameter in the system (1.5 times of particle diameter). The cells were used to determine the instantaneous and local volume fraction along the z direction. Initial values of the particle velocities were set to be zero.

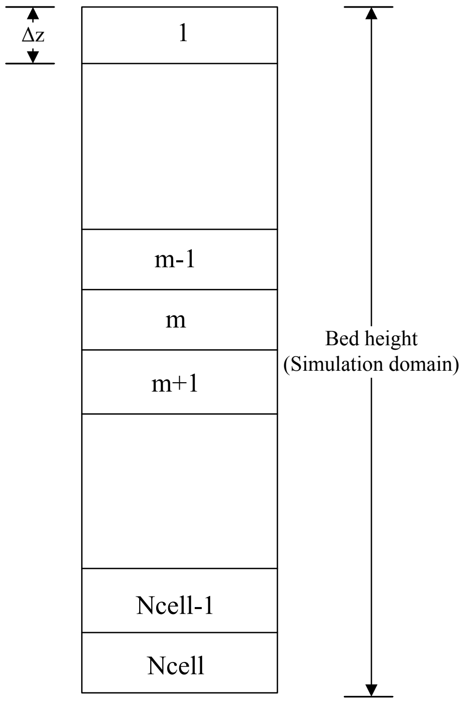

Figure 1: The simulation domain discretised into axial cells

A random fluid velocity drawn from the Gaussian PDF with the mean and standard deviation given by Eqs. 11-13 was associated to each particle at every updating interval which is defined following Crow et al. [28] approach and is about 0.01s. The standard deviation of the velocity distribution was a function of the fluid velocity and local volume fraction of the cell in which the particle centre was located. It is noted that based on PIV measurements, Reddy et al. [29] found that the axial fluid fluctuating velocity is 1.65 times that of the radial component and therefore we used that accordingly to find axial ${u^2}_{rms} = {u^2}_{rms,r} + {u^2}_{rms,z}$. This random fluid velocity was used to define the slip velocity and finally the drag force acting on each particle. Then, using a force balance (Eq. 7) along with the finite difference integration method (Eq. 9), the new position of the particle was defined. The flow chart of the simulation algorithm is schematically shown in figure 2.

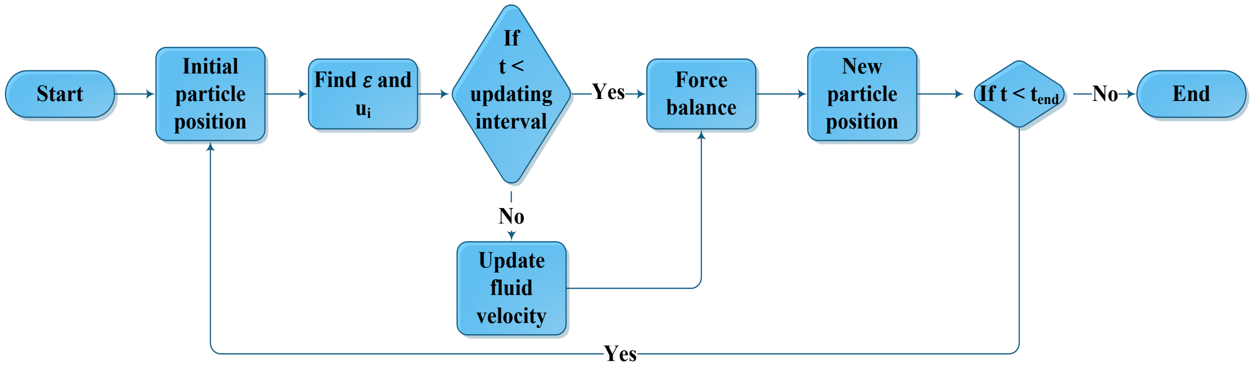

Figure 2: Schematic flow chart of simulation algorithm

The solid volume fraction of each cell is determined at any interval when the fluid fluctuating velocity and the drag coefficient are updated. Table 1 shows the required input parameters in the DEM simulations.

Table 1: Simulation input parameters

Properties	Value
Initial particle velocity (m/s)	0
Particle terminal velocity (m/s)	0.54
Minimum fluidization velocity (m/s)	0.06
No. of particles	201
Cell height (mm)	12
Liquid superficial velocity (m/s)	0.08-0.32
Stiffness (N/m)	100
Time step (s)	1×10^{-5}
Updating interval (s)	0.01
Coefficient of restitution	0.90
Richardson-Zaki index (n)	2.39

3.2 Granular pressure

In this paper, an attempt was made to numerically quantify the granular pressure in liquid solid fluidized beds using a method based on the KTGF definition of the granular pressure. In this method, the granular pressure was defined using the determination of particle-wall collision frequency and the corresponding particle momentum transport at the time of the collision. The momentum transport of the particles hitting the side wall of the cylindrical fluidized bed can be written as:

$$M_p = m\bar{v}(1+e) \tag{17}$$

The particle-wall collision frequency per unit area of the bed can also be defined as:

$$F_{p-w} = \frac{f_{p-w}}{A_s} = \frac{f_{p-w}}{\pi D_c h_e} \tag{18}$$

where h_e is the equilibrium bed height. Therefore, combining Eqs. 17 and 18, the granular pressure is defined as:

$$P_p = M_p F_{p-w} = \frac{m\bar{v}(1+e) f_{p-w}}{\pi D_c h_e} \tag{19}$$

4 RESULTS

4.1 Bed expansion

The well-known empirical correlation of Richardson and Zaki [1] was used to define the velocity-voidage relationship as:

$$u_{sf} = v_\infty \varepsilon_L^n \tag{20}$$

where n is the expansion index and v_∞ is the bed settling velocity at infinite dilution. Richardson and Zaki [1] suggested that the ratio of the bed settling velocity at infinite dilution to the single particle settling velocity in an infinite medium $\left(\frac{v_\infty}{v_t}\right)$ is a function of $\frac{d}{D_c}$ as:

$$v_\infty = v_t 10^{-\frac{d}{D_c}} \tag{21}$$

where v_t and D_c are the single particle settling velocity in an infinite medium and the column diameter, respectively. Figure 3 compares the simulation results of the liquid superficial velocity versus liquid volume fraction against the Richardson-Zaki [1] empirical equation. This figure illustrates that the simulation shows the same trend and in close agreement with the empirical correlation of Richardson and Zaki [1] for a wide range of liquid velocity and volume fraction. However, as can be seen, the behaviour of the fluidized bed in high voidage regions (approximately for ε_L > 0.85) is very complex [20, 30, 31]. As suggested by Eq. 21, $v_\infty < v_t$ and this makes the deviation of the simulation results at higher liquid volume fractions where the DEM results predict more realistically.

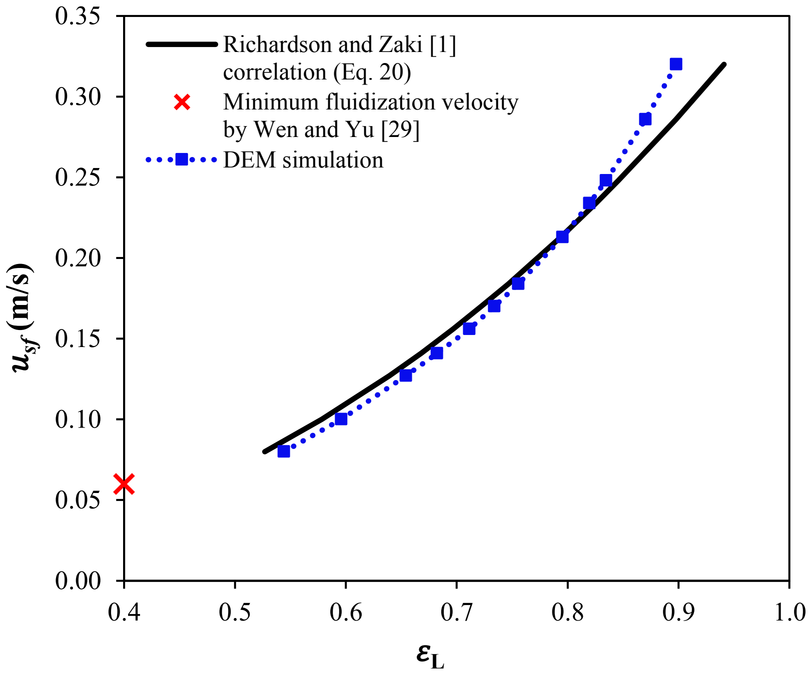

Figure 3: u_{sf} vs. ε_L; comparison of DEM simulation results to Richardson-Zaki [1] equation.

4.2 Granular temperature and pressure

Figure 4A and B shows the granular temperature and pressure versus solid volume fraction, respectively. Figure 4A exhibits a maximum at $\varepsilon_s \approx 0.1 - 0.2$. This also agrees with the experimental measurement of Zivkovic et al. [3] and simulation of Gervin et al. [4] that have reported the maximum granular temperature occurrence at $\varepsilon_s = 0.175$ and $\varepsilon_s \approx 0.1 - 0.2$, respectively.

Figure 4 B compares the DEM simulation results for the granular pressure using Eq. 19 to those obtained using the models proposed by Batchelor [5], Ding and Gidaspow [6] and Wang and Ge [12]. Our DEM results, Ding and Gidaspow [6] and Wang and Ge [12] models predict a maximum value in granular pressure for solid fractions of around 0.30-0.35, which is well in line with the reported experimental data by Zenit et al. [2] for high inertia particles. However, as can be seen, the maximum granular pressure calculated using Batchelor [5] model occurs at lower solid fraction of around 0.2 which also has been observed by experimental measurements of Zivkovic et al. [3] for high inertia particles.

Ghatage et al. [32] pointed out that this maximum value in the granular pressure might be a sign of a transition point from homogenous to heterogeneous regime. According to stability analysis, a fluidized bed can operate under either hydrodynamically stable or unstable condition depending upon the nature of dispersion [33].

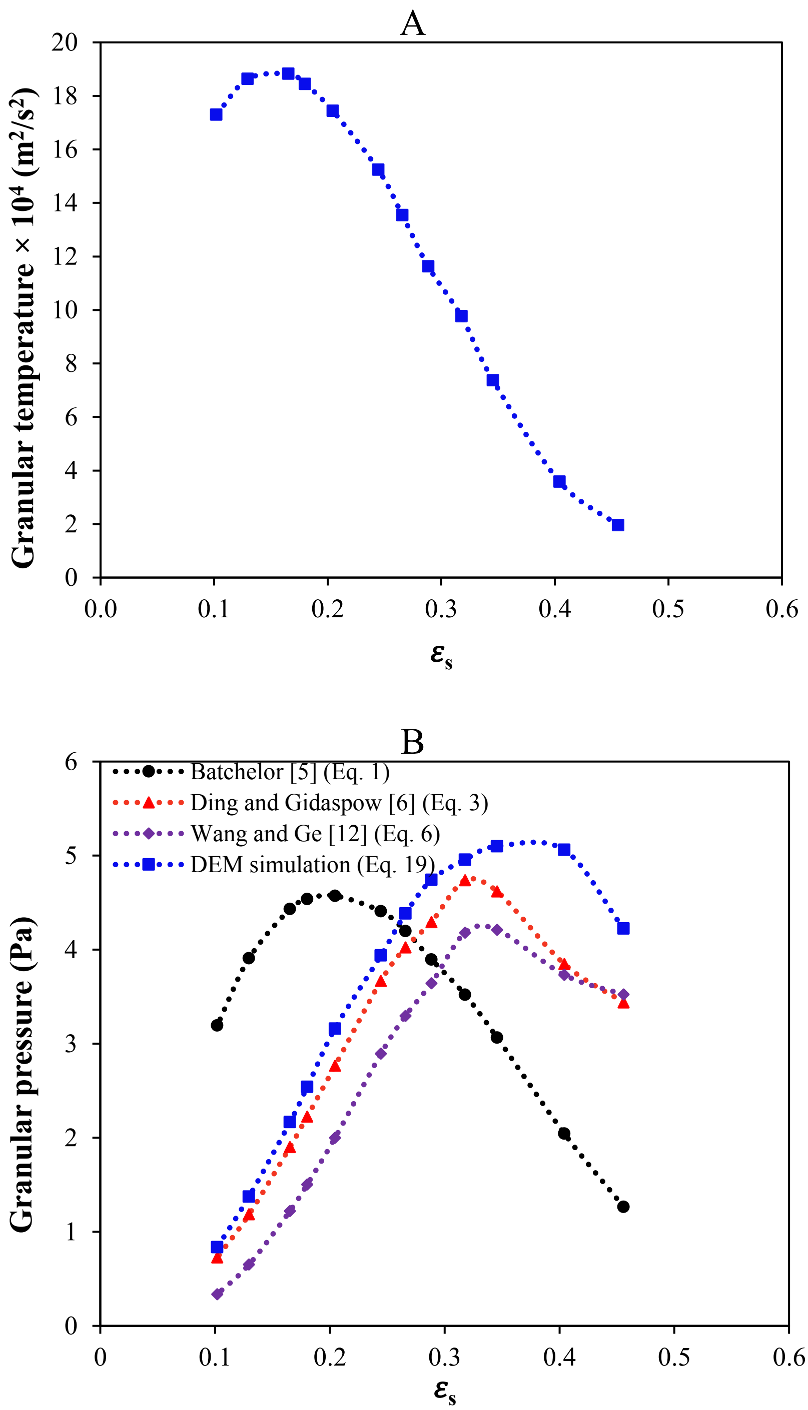

Figure 4: Granular temperature (A) and pressure (B) vs. solid volume fraction (ε_s).

Figure 5 shows the DEM simulation results for the collision to wall frequency versus solid volume fraction. Zenit et al. [2] claimed that at low concentrations, the value of the particle pressure is low as the particles are free to move and collision frequency is also smaller as shown in figure 5. On the other hand, at high solid fractions collisions are more likely to occur. However, very short mean free path of the particles causes these collisions to occur at very small velocities producing low-impulse collisions, which result in a low value of the particle pressure [2, 4]. Therefore, a combined effect of the higher impact velocity as well as the collision frequency results in higher granular pressure at intermediate concentrations (ε_s = 0.30-0.35).

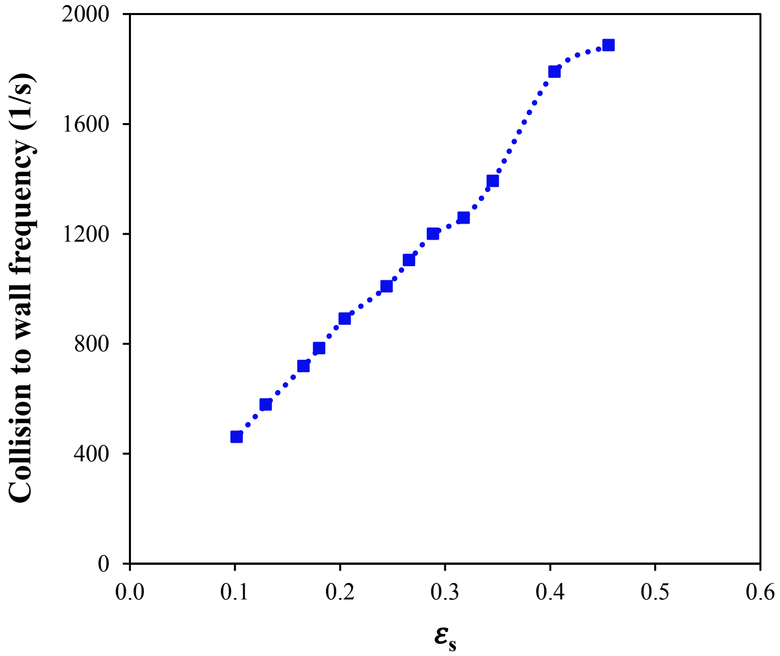

Figure 5: Collision to wall frequency (f_{p-w}) vs. solid volume fraction (ε_s).

7 CONCLUSION

In this study, a new DEM simulation approach has been used to simulate a liquid fluidized bed. A methodology based on the momentum transfer at the collision event was introduced to directly determine the granular pressure knowing the particle collision to wall frequency and speed.

In order to validate our DEM model, the bed expansion was compared to well-known Richardson-Zaki [1] equation where a good agreement was observed.

The granular pressure obtained by the DEM simulation then compared to some models available in literature. The quantity as well as the quality of the DEM results for the granular pressure agreed well with the majority of the current models. Similar peaks were observed in the intermediate concentration region (ε_s = 0.3-0.4) that is in line with the experimental observation of Zenit et al. [2] for the granular pressure in liquid fluidized beds.

Further stability analysis needs to be carried out in order to come to a rational conclusion whether that peak observed in the granular pressure values is related to any possible transition from homogeneous to heterogeneous regime in liquid fluidized beds.

REFERENCES

[1] Richardson, J.F. and Zaki W.N. Sedimentation and fluidisation. Part I. *Trans. lnstn Chem. Engrs.* (1954) **32**:35-53.

[2] Zenit, R., Hunt, M.L. and Brennen, C.E. Collisional particle pressure measurements in solid-liquid flows. *J. Fluid. Mech.* (1997) **353**:261-283.

[3] Zivkovic, V., Biggs, M.J. and Glass, D. Granular Pressure in a Liquid-Fluidized Bed as Revealed by Diffusing Wave Spectroscopy. *AIChE J.* (2012) **58**:1069-1075.

[4] Gevrin, F., Masbernata, O. and Simonin, O. Granular pressure and particle velocity fluctuation prediction in liquid fluidized beds. *Chem. Eng. Sci.* (2008) **63**:2450-2464.

[5] Batchelor, G.K. A new theory of the instability of a uniform fluidized bed. *J. Fluid. Mech.* (1988) **193**:75-110.

[6] Ding, J., Gidaspow, D. A bubbling fluidization model using kinetic theory of granular flow. *AIChE J.* (1990) **36**(4):523-538.

[7] Gidaspow, D. *Multiphase flow and fluidization: continuum and kinetic theory descriptions*. Academic press, (1994).

[8] Abbasfard, H., Evans, G. and Moreno-Atanasio, R. Effect of van der Waals force cut-off distance on adhesive collision parameters in DEM simulation. *Powder Technol.* (2016) **299**:9-18.

[9] Bagnold, R.A. Experiments on a gravity-free dispersion of large solid spheres in a Newtonian fluid under shear. Proc R Soc London Ser A. (1954) **225**:49-63.

[10] Carnahan, N.F. and Starling, K.E. Equation of state for non-attracting rigid spheres. *J. Chem. Phys.* (1969) **51**:635-636.

[11] Lun, C. and Savage, S. The effects of an impact velocity dependent coefficient of restitution on stresses developed by sheared granular materials. *Acta Mech.* (1986) **63**:15-44.

[12] Wang, J. and Ge, W. Collisional particle–phase pressure in particle–fluid flows at high particle inertia. *Phys. Fluids*. (2005) **17**:128103.

[13] Cundall, P.A. and Strack, O.D. A discrete numerical model for granular assemblies. *Geotechnique.* (1979) **29** (1):47-65.

[14] Di Felice, R. The voidage function for fluid-particle interaction systems. *Int. J. Multiphase Flow.* (1994) **20**(1):153-159.

[15] Kafui, K., Thornton, C. and Adams, M. Discrete particle-continuum fluid modelling of gas–solid fluidised beds. *Chem. Eng. Sci.* (2002) **57**(13):2395-2410.

[16] Clift, R., Grace, J.R. and Weber, M.E. *Bubbles, drops, and particles*: Courier Corporation, (2005).

[17] Handley, D., A D, Butcher, K. and Franklin N. A study of fluid and particle mechanics in liquid-fluidised beds. *TRANSACTIONS OF THE INSTITUTION OF CHEMICAL ENGINEERS AND THE CHEMICAL ENGINEER.* (1966) **44**(7):T260.

[18] Carlos, C. and Richardson, J. Solids movement in liquid fluidised beds—I Particle

velocity distribution. *Chem. Eng. Sci.* (1968) **23**(8):813-824.
[19] Latif, B. and Richardson, J. Circulation patterns and velocity distributions for particles in a liquid fluidised bed. *Chem. Eng. Sci.* (1972) **27**(11):1933-1949.
[20] Đuriš, M., Radoičić, T.K., Garić-Grulović, R., Arsenijević, Z. and Grbavčić, Ž. Particle velocities in quasi two-dimensional water fluidized beds of spherical particles. *Powder Technol.* (2013) **246**:98-107.
[21] Hinze, J. *Turbulence*. McGraw-Hill. *New York.* (1975).
[22] Pozorski, J. and Minier, J-P. On the Lagrangian turbulent dispersion models based on the Langevin equation. *Int. J. Multiphase Flow.* (1998) **24**(6):913-945.
[23] Doroodchi, E., Evans, G., Schwarz, M., Lane, G., Shah, N. and Nguyen, A. Influence of turbulence intensity on particle drag coefficients. *Chem. Eng. J.* (2008) **135**(1):129-134.
[24] Bel Fdhila, R. and Simonin, O. Eulerian prediction of a turbulent bubbly flow downstream of a sudden pipe expansion. Paper presented at: Proceedings 5th Workshop on Two-Phase Flow Predictions (1992).
[25] Spelt, P. and Biesheuvel, A. On the motion of gas bubbles in homogeneous isotropic turbulence. *J. Fluid. Mech.* (1997) **336**:221-244.
[26] Lali, A., Khare, A., Joshi, J. and Nigam, K. Behaviour of solid particles in viscous non-Newtonian solutions: settling velocity, wall effects and bed expansion in solid-liquid fluidized beds. *Powder Technol.* (1989) **57**(1):39-50.
[27] Wen, C. and Yu, Y. A generalized method for predicting the minimum fluidization velocity. *AIChE J.* (1966) **12**(3):610-612.
[28] Crowe, C. An assessment of multiphase flow models for industrial applications. Paper presented at: Proceeding of FEDSM (1998).
[29] Reddy, R., Sathe, M., Joshi, J., Nandakumar, K. and Evans, G. Recent developments in experimental (PIV) and numerical (DNS) investigation of solid–liquid fluidized beds. *Chem. Eng. Sci.* (2013) **92**:1-12.
[30] Epstein, N. *Liquid Solids Fluidization*, in: W.C. Yang (Ed.), Handbook of fluidization and fluid-particle systems, Marcel Dekker, New York, (2003) 705-764.
[31] Di Felice, R. Liquid suspensions of single and binary component solid particles – an overview, *China Part.* (2007) **5**:312–320.
[32] Ghatage, S.V., Peng, Z., Sathe, M.J., et al. Stability analysis in solid–liquid fluidized beds: experimental and computational. *Chem. Eng. J.* (2014) **256**:169-186.
[33] Joshi, J.B., Deshpande, N.S., Dinkar, M. and Phanikumar, D.V. Hydrodynamic stability of multiphase reactors. *Adv. Chem. Eng.* (2001) **26**: 1-130.